SLAC-PUB--3891
DE86 009781

WAKE FIELD ACCELERATORS*

P. B. WILSON

Stanford Linear Accelerator Center
Stanford University, Stanford, California, 94305

Invited talk presented at the SLAC Summer Institute on Particle Physics, Stanford, California, July 29 – August 9, 1985

* Work supported by the Department of Energy, contract DE – AC03 – 76SF00515.

1. Introduction

In a wake field accelerator a high current driving bunch injected into a structure or plasma produces intense induced fields, which are in turn used to accelerate a trailing charge or bunch. The driving bunch and the accelerated bunch may or may not follow the same path through the structure. An important concept is the so-called transformer ratio. The driving bunch induces a retarding field within the bunch as the kinetic energy of the bunch is transformed into electromagnetic energy in the wake field. The maximum absolute value of this retarding field is denoted by E_m^-. The transformer ratio is then $R \equiv E_m^+/E_m^-$, where $E_m^+ = E_a$ is the maximum accelerating gradient seen by a test charge moving behind the driving bunch on the same or on a parallel path. The retarding and accelerating fields are assumed to be averaged over the length of the structure, or over one period if the structure is periodic.

In a sense, almost all accelerators are wake field accelerators. For example, in a conventional rf-driven accelerator a high current, low voltage beam induces an rf voltage in the output cavity of a klystron. The induced electromagnetic wave (the wake field) then travels through a waveguide to the accelerating structure. In this lecture, however, we consider only wake field acceleration in the conventional sense, in which a driving bunch is injected into a metallic cavity or structure. A close relative of this type of wake field accelerator is the plasma wake field accelerator. In this device a driving bunch is injected into a plasma, setting up strong longitudinal plasma oscillations which can be used to accelerate a following bunch. The plasma wake field accelerator is treated elsewhere in these proceedings.[1]

2. Basic Concepts

Consider a point charge q moving in free space with a velocity close to that of light. The electric and magnetic field lines will lie nearly in a transverse plane, with an opening angle given approximately by $1/\gamma$. Suppose now that the charge moves past a perturbing metallic obstacle, which is displaced from the path of the charge by a distance b as shown in Fig. 1, and that it passes the point $z = 0$ at $t = 0$. Scattered radiation will tend to fill in behind an expanding spherical wavefront, traveling at the velocity of light, as shown schematically in the figure. Suppose a test particle follows the same path along the z axis as the driving charge q, but at a fixed distance s behind. At time $t \approx (b^2 + s^2)/2cs$, the scattered field will begin to reach the axis at position $z_c = z_q - s$ producing both longitudinal and transverse forces acting on the test particle. The intensity of the forces due to these "wake fields" is proportional to the magnitude of the driving charge. Furthermore, the wake field forces can be greatly enhanced by entirely surrounding the axis with an appropriately shaped metallic boundary. The driving charge can in addition be a shaped charge distribution, and the test charge need not follow the same path as the driving charge.

The goal of wake field accelerator design is to adjust the structure geometry, the shape of the driving charge distribution and the paths of the driving and accelerated charges to strike an optimum balance among the following four quantities:

$$R \equiv \frac{E_a}{E_m^-} \tag{1}$$

$$\eta = \frac{u}{qE_m^-} \tag{2}$$

$$k_\ell \equiv \frac{E_a^2}{4u} \tag{3}$$

$$k_a \equiv \frac{E_a}{2q} = \frac{2\eta k_\ell}{R} \tag{4}$$

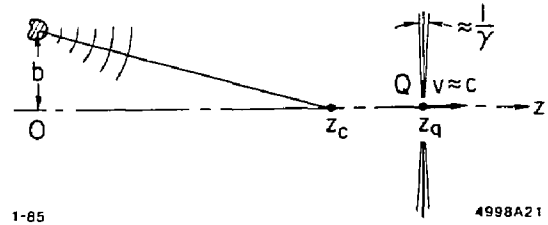

Figure 1. Figure showing the radiation field from a perturbing metallic object excited by the field of a relativistic charge moving along the z-axis.

Given a driving bunch in which all the electrons have the same energy eV_0, then Eq. (1) states that the maximum energy that can be attained by an electron following behind the driving bunch is eRV_0, assuming electrons in the driving bunch which experience the maximum retarding field are just brought to rest. Equation (2) is the efficiency for the transfer of energy from the driving bunch to energy u per unit length of structure in the wake fields. Equation (3) is a figure of merit for the conversion of field energy per unit length into accelerating gradient. The parameter k_ℓ scales inversely as the square of the transverse dimensions of the structure. In Eq. (4) k_u is another figure of merit giving the accelerating gradient produced per unit driving charge. Note that it is inconsistent to have both a high transformer ratio and a large k_u. A third loss parameter can also be defined: $k_u \equiv u/q^2$. The three loss parameters are related by $k_z^2 = k_\ell k_u$. For a single rf mode $k_\ell = k_z = k_u$, and all three loss parameters are identically equal to the rf loss parameter as usually defined.

Let us next consider the wake fields set up by some simple metallic boundary discontinuities having cylindrical symmetry. In Fig. 2(a) a charge moving in free space at $v \approx c$ enters along the axis of a section of perfectly conducting pipe with infinitely thin walls. The field lines are not perturbed by the pipe in the limit $\gamma \to \infty$, either upon entering or leaving, and consequently no wake fields are produced. The situation is different for the configuration shown in Fig. 2(b). Here it is assumed that the fields from the charge have been confined inside the pipe for $z < 0$. As the charge exits from the pipe at $z = 0$, a toroidal radiation field is set up as shown by the dashed lines. The surface charge splits into two portions, a charge Q_1 on the outside of the pipe and a charge Q_2 on the inside, with $Q_1 + Q_2$ equal to the driving charge Q. The initial ratio Q_2/Q_1 can be determined by minimising the energy in the radiation field,[2] giving in this case $Q_1 = Q_2 = Q/2$. However, computer simulations on similar problems indicate that the radiation field may not be confined to a delta-function wavefront expanding at the velocity of light, but rather might be smeared out over the region behind the wavefront in a complicated way. In addition, the ratio Q_2/Q_1 does not seem to remain

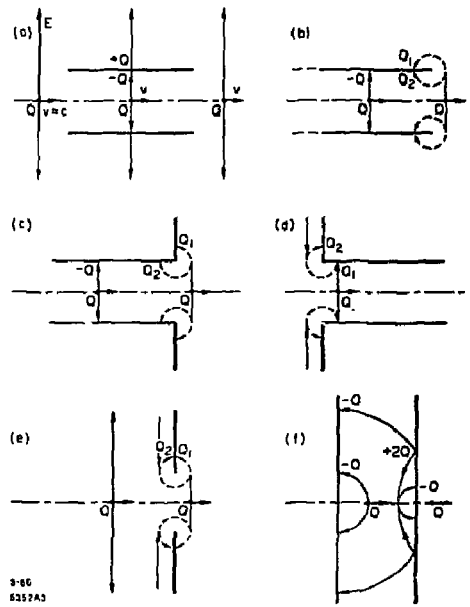

Figure 2. Fields excited by a point charge moving with $v \approx c$ past several cylindrically symmetric discontinuities.

constant in time. Very probably, the total charge on the inside of the pipe decreases with increasing time. This seemingly simple boundary value problem has not, however, been solved analytically.

Figures 2(c), 2(d) and 2(e) show some additional elementary geometries, with their associated toroidal wake fields. Again, it should be emphasized that these apparently elementary boundary value problems have not been solved analytically. The details of the radiation field, indicated only schematically by the dashed lines, are in fact the subject of some controversy. Hand-waving arguments have been used to prove that the radiation field is, or is not, confined to a sharp wavefront. It has also been argued[3] that in these three cases there are no wake fields at all in the region $r < a$, where a is the radius of the aperture.

The situation is different for the case of Fig. 2(f), which shows a point charge passing between two parallel metallic plates. This case is important in that two parallel planes give the same wake fields as a pillbox cavity for distances behind the driving charge such that $s < s_0$ where

$$s_0 = (g^2 + 4b^2)^{1/2} - g \quad .$$

Here b is the cavity radius and g the gap spacing between the faces of the pillbox. In other words, if $s < s_0$ the signal induced by a driving charge as it enters through the first face of the pillbox can propagate to the outer cylindrical wall, be reflected, and return to the axis to influence a trailing test charge before the test charge exits through the second face of the pillbox. The pillbox cavity is important because it can often serve as a primitive model for an accelerating structure. The wake fields for the case of Fig. 2(f) have been calculated analytically (see, for example, Ref. 4).

Of course, the detailed behavior of the wake fields in time and space is not the feature of main interest. What we really want to know is the net energy gain or the net transverse kick integrated through a structure for a test particle following at a fixed distance behind the driving charge, assuming that both the

driving charge and the test particle are traveling at $v \approx c$. The longitudinal wake potential per unit driving charge is then defined by

$$W_z(s) = -\frac{1}{q}\int_{z_1}^{z_2} dz \; [E_z(z,t)]_{t=(z+s)/c} \qquad (5a)$$

assuming both driving and test charges are traveling parallel to the z axis. Here $z_2 - z_1$ is the region over which the wake fields are appreciable for a finite structure, or the periodic length for a periodic structure. A similar expression holds for the transverse wake potential:

$$\mathbf{W}_\perp(s) = \frac{1}{q}\int_{z_1}^{z_2} dz \; [\mathbf{E}_\perp + (\mathbf{v}\times\mathbf{B})_\perp]_{t=(z+s)/c} \quad . \qquad (5b)$$

In the above expressions the position of the driving charge is assumed to be $z = ct$, and the wake fields are integrated in a frame of reference moving with the test particle.

As mentioned above, analytic expressions have been obtained for the wake fields (the transition radiation) generated by a point charge entering and leaving the region between two parallel metallic planes. Using the E_z field component derived in Ref. 4, K. Bane[5] has carried out the integration in Eq. (5a) to obtain the delta function wake potential for this case:

$$2\pi\epsilon_0 W_z(s) = 2\delta(s)\,\ln\left[\frac{g}{s}\right] - 2\sum_{n=1}^{\infty}\delta(2ng-s)\,\ln\left[\frac{s^2}{(s+g)(s-g)}\right] - \frac{1}{2}\left\{\frac{1}{\left[\frac{s}{2g}\right]_{IP}+\frac{s}{2g}} - \frac{1}{\left[\frac{s}{2g}\right]_{IP}+\frac{s}{2g}+1}\right\} \quad . \qquad (6)$$

Here g is the separation between the planes and IP means the integer part of the term in brackets. This function is shown in Fig. 3. Note that the wake

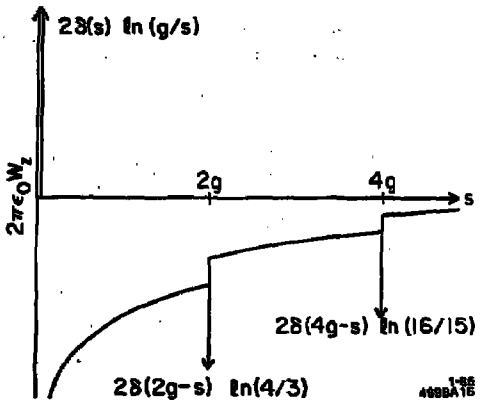

Figure 3. Longitudinal delta-function wake potential for a point charge moving perpendicular to two parallel metallic planes.

is accelerating ($W_z < 0$) for all $s > 0$. However, the wake seen by the driving charge itself at $s = 0$ is retarding, and the transformer ratio as defined previously is always less than one.

A similar situation is encountered in the case of a point driving charge moving at $v \approx c$ on the axis of a hollow tube with resistive walls. Again, the wake is accelerating behind the driving charge, except for a very small region within a critical distance (.01 mm for a point charge moving in copper tube 8 cm in radius) immediately behind the charge. It can be shown that for such a resistive wall tube the transformer ratio is less than $1/\sqrt{\pi}$ (see Ref. 6, Sec. 3.2).

Once the wake potential for a unit point charge is known, the potential at any point within or behind an arbitrary charge distribution with line density $\rho(s)$ can be computed by

$$V(s) = -\int_{s}^{\infty} W_z(s' - s)\, \rho(s')\, ds' \quad . \tag{7}$$

The total loss parameter k_u is then obtained from

$$k_u = \frac{1}{q^2} \int_{-\infty}^{\infty} V(s)\, \rho(s)\, ds \quad . \tag{8}$$

3. Wake Potentials for Closed Cavities and Periodic Structures

Consider a driving charge Q moving at velocity $\mathbf{v}$ through a closed cavity with perfectly conducting walls, as shown in Fig. 4. A test charge also moves at the same velocity, but on a path which parallel to that of the driving charge and at a longitudinal distance s behind. Our goal is to calculate the longitudinal and transverse wake potentials experienced by the test charge in the limit $v \approx c$. For $v \not\approx c$ the expressions for the wake potentials are in general much more complicated and the wake potential concept is less useful.

Under certain rather general conditions, which will be spelled out in detail later, it can be shown[6,7] that the longitudinal and transverse wake potentials can be written in terms of the properties of the normal modes of the charge-free cavity in a relatively simple way:

$$W_z(\mathbf{r}',\mathbf{r},s) = 2H(s)\sum_n k_n(\mathbf{r}',\mathbf{r})\cos\frac{\omega_n s}{c} \tag{9a}$$

$$\mathbf{W}_\perp(\mathbf{r}',\mathbf{r},s) = 2H(s)\sum_n k_{n\perp}(\mathbf{r}',\mathbf{r})\sin\frac{\omega_n s}{c} \tag{9b}$$

where

$$H(s) \equiv \begin{cases} 0 & s<0 \\ 1/2 & s=0 \\ 1 & s>0 \end{cases}$$

and

$$k_n(\mathbf{r}',\mathbf{r}) = \frac{V_n^*(\mathbf{r}')\,V_n(\mathbf{r})}{4U_n} \tag{10a}$$

$$k_{n\perp}(\mathbf{r}',\mathbf{r}) = \frac{V_n^*(\mathbf{r}')\,\nabla_\perp V_n(\mathbf{r})}{4U_n\omega_n/c} \quad . \tag{10b}$$

Here ω_n is the angular frequency the nth mode, and $V_n(\mathbf{r})$ is the voltage that would be gained by a nonperturbing test particle crossing the cavity in which

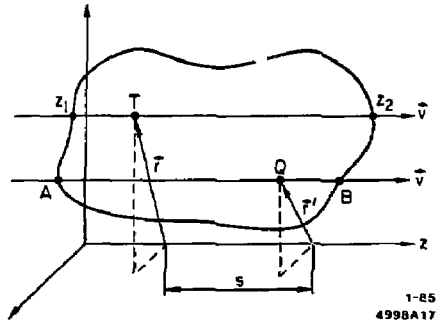

Figure 4. A driving charge Q, moving at constant velocity $\mathbf{v}$ parallel to the z-axis, enters a closed cavity at A $(\mathbf{r}', z=0)$ at $t=0$ and leaves at B $(\mathbf{r}', z=L)$. A non-perturbing test particle T also moves at the same velocity $\mathbf{v}$, but at transverse position $\mathbf{r}$ and at longitudinal distance s behind Q.

energy U_n is stored in the nth mode. Assuming the electric field for the n^{th} mode varies with time as $\exp(i\omega t)$ and the position of the test particle is given by $z = ct$, this voltage is

$$V_n(\mathbf{r}) = \int_{z_1}^{z_2} dz\ E_z(\mathbf{r}, z)\ \exp\left(\frac{i\omega_n z}{c}\right) \quad . \tag{11}$$

The conditions under which Eqs. (9) are valid for the longitudinal and transverse wake functions are discussed in detail in Refs. 6 and 7, and are summarized in Table I. We see that if the driving charge and test particle follow different paths in a closed cavity of arbitrary shape, neither Eq. (9a) nor (9b) give a valid description of the wake potentials. If the particles follow the same path in a closed cavity of arbitrary shape, Eq. (9a) is valid for the longitudinal wake potential but Eq. (9b) does not correctly describe the transverse wake potential. Formal expressions can indeed be written down for the non-valid cases, but the integrals are much more complicated, and the wake potentials for a given mode do not separate neatly into a product of an s-dependent factor and a factor which depends only on $\mathbf{r}$.

Note that Eqs. (9a) and (9b) are related by

$$\frac{\partial \mathbf{W}_\perp}{\partial s} = \nabla_\perp W_z \quad . \tag{12}$$

This relation between the longitudinal and transverse wakes is sometimes termed the Panofsky-Wenzel theorem.[8] It was originally derived to calculate the transverse momentum kick received by a nonperturbating charge traversing a cavity excited in a single rf mode.

The wake potential formalism, using properties of the charge-free cavity modes, makes it possible to calculate useful quantities for the charge-driven cavity. An important example is the longitudinal wake potential for the case in

Table I

Cases for which Eqs. (9a) and (9b) give the wake potentials in the limit $v \approx c$

Case	Eq. (9a) Valid for W_z	Eq. (9b) Valid for $\mathbf{W}_\perp$
(a) Test charge and driving charge follow different paths in a closed cavity of arbitrary shape.	No	No
(b) Test charge and driving charge follow the same path in cavity of arbitrary shape.	Yes	No
(c) Velocity v is in the direction of symmetry of a right cylinder of arbitrary cross section.	Yes	Yes
(d) Both driving charge and test charge move in the beam tube region of an infinite repeating structure of arbitrary cross section.	Yes	Yes
(e) Both particles move near the axis of any cylindrically symmetric cavity.	Yes	Yes

which the test charge and driving charge follow the same path. Equations (9a) and (10a) reduce to

$$W_z(\mathbf{r}, s) = \sum_n k_n(\mathbf{r}) \cos\frac{\omega_n s}{c} \times \begin{cases} 0 & s < 0 \\ 1 & s = 0 \\ 2 & s > 0 \end{cases} \tag{13}$$

$$k_n(\mathbf{r}) = \frac{|V_n(\mathbf{r})|^2}{4U_n} \quad .$$

The potential seen by the charge itself is

$$V(\mathbf{r}, 0) = -q\, W_z(\mathbf{r}, 0) = -q \sum_n k_n(\mathbf{r}) \tag{14a}$$

$$V_n(r,0) \equiv V_n(0) = -q\,k_n \quad . \tag{14b}$$

The energy left behind in the n^{th} mode after the driving charge has left the cavity is

$$U_n = -q\,V_n(0) = q^2\,k_n \quad . \tag{15}$$

The parameter k_n is the constant of proportionality between the energy lost to the nth mode and the square of the driving charge, hence the name loss parameter or loss factor.

Note from Eq. (13) that an infinitesimal distance behind a driving point charge the potential is retarding for the nth mode with magnitude

$$V_n(0^+) = 2V_n(0) = -2q\,k_n \quad . \tag{16a}$$

As a function of distance s behind the driving charge, the potential varies as

$$V_n(s) = V_n(0^+)\cos\frac{\omega_n s}{c} = -2q\,k_n\cos\frac{\omega_n s}{c} \quad . \tag{16b}$$

Equation (16a) expresses what is sometimes termed the fundamental theorem of beam loading[9]: the voltage induced in a normal mode by a point charge is exactly twice the retarding voltage seen by the charge itself. The transformer ratio for a point charge exciting a single mode is then also exactly equal to two. It is readily shown that this factor of two follows directly from conservation of energy.[9] In Sec. 4 we will show that this restriction on the transformer ratio for a point charge does not necessarily apply to an extended driving charge distribution.

A physical wake for a real cavity is a summation over many modes. Perhaps the modes might add up to produce a transformer ratio greater than two, even for a point charge. We note, however, that the wake for each mode varies with s as $W_n = 2k_n\cos(\omega_n s/c)$. At $s = 0^+$ the wakes all add in phase, and the sum of the wakes for all the modes gives a retarding potential which is exactly twice

the retarding potential seen by the driving charge itself at $s = 0$. At any value of s where the net wake is accelerating, the cosine wakes for the individual modes can never do better than add exactly together in phase, as they do at $s = 0^+$. Thus

$$|W(s)| \le \sum_n W_n(s = 0^+) = 2\sum_n W_n(s = 0) \quad , \tag{17}$$

and the transformer ratio for a real cavity with many modes, driven by a point charge, is equal to or less than two. In practice it will be considerably less than two, since the modes will never come close to adding in phase anywhere except at $s = 0^+$.

It is easy to show that Eq. (17) also follows from conservation of energy. Consider a point driving charge q_1 which loses energy

$$U_1 = q_1^2\,W(0) \tag{18a}$$

to the wake fields in a cavity (remember that $W(0)$ is always positive by definition). The accelerating potential at position s is $-q_1W(s)$. By superposition the energy gained by a charge q_2 at position s is

$$U_2 = -q_2\,|q_1\,W(s) + q_2\,W(0)| \quad . \tag{18b}$$

Assume first that q_1 and q_2 have the same sign. By conservation of energy $U_2 \le U_1$, and using Eqs. (18a) and (18b) the transformer ratio $R = -W(s)/W(0)$ is

$$R \le \frac{q_1^2 + q_2^2}{q_1\,q_2} = \frac{1+\alpha^2}{\alpha}$$

where $\alpha \equiv q_2/q_1$ is positive. This inequality must hold for any value of α, in particular for $\alpha = 1$ which minimizes the right-hand side, leading to $R \le 2$. If q_1 and q_2 are opposite in sign, the transformer ratio is redefined as $R' = -R$, α is replaced by $-|\alpha|$, and the above expression again gives $R' \le 2$.

If the driving charge and the accelerated charge follow different paths through the cavity, the situation becomes more complicated. We first note from Eqs. (9) and (10) that the longitudinal wake potential is unchanged if the paths of the driving charge and the test charge are interchanged. This symmetry with respect to the interchange of $\mathbf{r}$ and $\mathbf{r}'$ is also an alternative expression of the Lorentz reciprocity theorem, derived in standard texts on microwave theory.[10] If we now apply conservation of energy to two charges q_1 and q_2 following different paths, we can show that

$$|W_{12}(s)| = |W_{21}(s)| \leq 2\,[W_1(0)\ W_2(0)]^{1/2} \quad , \tag{19}$$

where $W_{12}(s)$ is the wake along path 2 produced by a charge travelling on path 1, and so forth. If we define a transformer ratio R_{12} by

$$R_{12}(s) \equiv \frac{|W_{12}(s)|}{W_1(0)}$$

and similarly for R_{21}, then for any value of s

$$R_{12} \leq 2\left[\frac{W_2(0)}{W_1(0)}\right]^{1/2} = 2\left[\frac{\sum_n k_n(r_2)}{\sum_n k_n(r_1)}\right]^{1/2} \tag{20a}$$

$$R_{21} \leq 2\left[\frac{W_1(0)}{W_2(0)}\right]^{1/2} = 2\left[\frac{\sum_n k_n(r_1)}{\sum_n k_n(r_2)}\right]^{1/2} \tag{20b}$$

and

$$R_{12}\ R_{21} \leq 4 \quad . \tag{20c}$$

The case of a periodically repeating structure is of obvious importance in accelerator design. Although real periodic structures are of course never infinite, practical structures at least a few periods in length seem to fulfill condition (d) of

Table I. Thus the wake potentials can be computed by a summation over normal modes. For the case of a cylindrically symmetric structure, all modes depend on the azimuthal angle ϕ as $e^{im\phi}$. The wake potentials can then be written[6] for $s > 0$,

$$W_{zm} = 2\left(\frac{r'}{a}\right)^m \left(\frac{r}{a}\right)^m \cos m\phi \sum_n k_{mn}^{(a)} \cos\frac{\omega_{mn}s}{c} \tag{21a}$$

$$W_{\perp m} = 2m\left(\frac{r'}{a}\right)^m \left(\frac{r}{a}\right)^{m-1} \left(\hat{r}\cos m\phi - \hat{\phi}\sin m\phi\right) \times \sum_n \frac{k_{mn}^{(a)}}{\omega_{mn}a/c} \sin\frac{\omega_{mn}s}{c} \quad . \tag{21b}$$

Here $\hat{r}$ and $\hat{\phi}$ are unit vectors and $k_{mn}^{(a)}$ is the loss factor per unit length calculated at $r = a$, where a is the radius of the beam tube region. That is

$$k_n^{(a)} \equiv \frac{[E_{zn}(r=a)]^2}{4u_n}$$

where u_n is the energy per unit length in the n^{th} mode. The longitudinal cosine-like wake potential per period for the SLAC structure is shown in Fig. 5. Note the very rapid fall-off in the wake immediately behind the driving charge, from a peak wake of 8 V/pC per period at time $t = s/c = 0^+$. The wake seen by a point charge would be just one half of this wake, or 4 V/pC. The sine-like tranverse dipole ($m = 1$) wake potential for the SLAC structure is shown in Fig. 6. This figure illustrates the fact that the total wake potential is obtained by summing a finite number of modes that can be obtained using a reasonable computation time, and then adding on a so-called analytic extension to take into account the contribution from very high frequency modes. Details are discussed in Ref. 11.

If the dimensions of a particular structure are scaled by a factor F, the frequencies of the normal modes scale as F^{-1}. The amplitude of the longitudinal wake potential *per unit length of structure* scales as F^{-2} at time Ft, or in terms

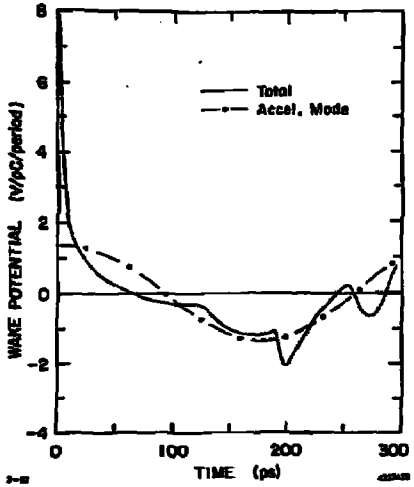

Figure 5. Longitudinal delta-function wake potential per cell for the SLAC disk-loaded accelerator structure.

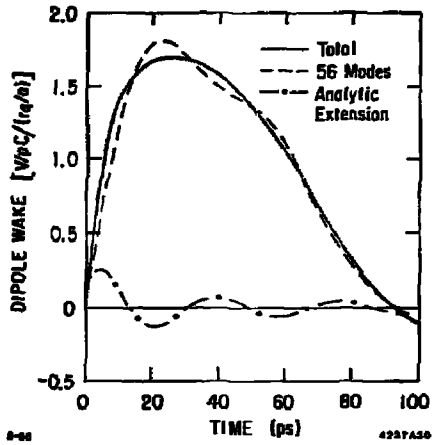

Figure 6. Dipole delta-function wake potential per cell for the SLAC structure.

of the modal frequencies as ω_n^2. The amplitude of the dipole wake potential per unit length at time Ft scales as F^{-3}, or as ω_n^3.

4. Wake Potentials on a Collinear Path with a Charge Distribution

In the last section, the wake potentials due to a point driving charge traversing a closed cavity were considered under rather general conditions. In this section we confine our attention to the case in which the driving charge and test particle *follow the same path* through a cavity or structure, but we allow the driving charge to be a distribution such that the line density is given by $\rho(s) = I(t)/c$. The potential at time $t = s/c$ is then

$$V(t) = -\int_{-\infty}^{t} I(t')\, W_s(t-t')\, dt' \quad . \tag{22}$$

For a point charge we found previously that

$$V(t) = -2q\sum_n k_n \cos\omega_n t \quad .$$

If such a charge having initial energy qV_0 is just brought to rest by the retarding wake potential at $t = 0$, then $V_0 = q\sum_n k_n$ and

$$V(t) = -\frac{2V_0\sum_n k_n \cos\omega_n t}{\sum_n k_n} \quad . \tag{23}$$

If the structure supports only a single mode, then $V(t) = -2V_0\cos\omega_n t$. However, a physical bunch, even a very short bunch, consists of a large number of individual charges which are not rigidly connected. Thus the leading charge in such a physically real bunch will experience no deceleration, while the trailing charge will experience the full induced voltage, or twice the average retarding voltage

per particle (assuming the bunch length is short compared to the wavelengths of all modes with appreciable values of k_n). The wake potential for a short charge distribution extending from $t = 0$ to $t = T$, interacting with a single mode, is illustrated in Fig. 7(a). Within the bunch the potential is given by

$$V(t) = -\frac{2V_0}{q}\int_0^t I(t')\, dt' \quad , \tag{24}$$

where V_0 is the average energy loss per particle in the distribution. This can be seen by substituting Eq. (24) in

$$V_0 = \overline{V}(t) = \frac{1}{q}\int_0^T V(t)\, I(t)\, dt \quad ,$$

and working out the double integral. Note from Eq. (24) that for $t = T$ at the end of the distribution $V(T) = -2V_0$. Therefore $V_m^+ = 2V_0$, $V_m^- = |-2V_0| = 2V_0$ and the transformer ratio is $R = V_m^+/V_m^- = 1$.

The potential in and behind a long charge distribution is shown schematically in Fig. 7(b). We consider first the case for a single mode. From Eq. (22) with $W_s(t) = 2k_n\cos\omega_n t$,

$$V_n(t) = -2k_n\int_{-\infty}^{t} I(t')\, \cos\omega_n(t-t')\, dt' \quad . \tag{25}$$

Assume now that the bunch extends in time from $-T$ to $+T$. Within the bunch $(-T < t < T)$ the retarding potential is

$$V_n^-(t) = -2k_n\left[\cos\omega_n t\int_{-T}^{t} I(t')\cos\omega_n t'\, dt' + \sin\omega_n t\int_{-T}^{t} I(t')\sin\omega_n t'\, dt'\right] . \tag{26}$$

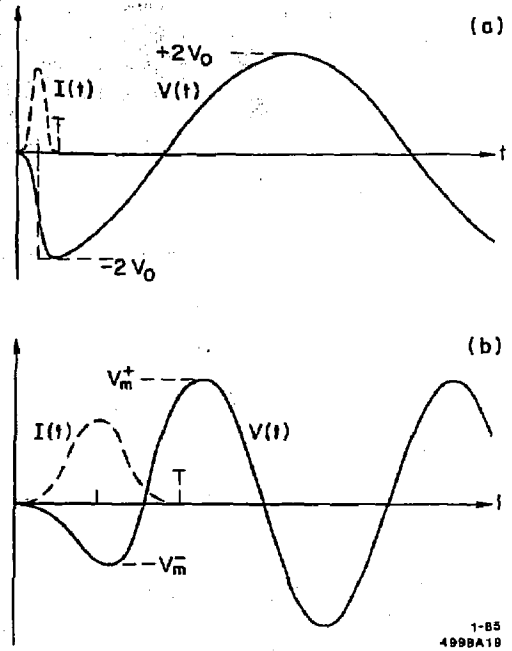

Figure 7. Potential in and behind a charge distribution interacting with a single mode for (a) a *short* bunch, and (b) a *long* bunch.

Following the bunch ($t > T$) the accelerating potential is

$$V_n^+(t) = 2k_n \left[\cos\omega_n t \int_{-T}^{T} I(t') \cos\omega_n t' \, dt' + \sin\omega_n t \int_{-T}^{T} I(t') \sin\omega_n t' \, dt' \right] . \quad (27)$$

If the bunch is symmetric about $t = 0$, the second integral in Eq. (27) vanishes, and $V^+(t)$ reaches a maximum value given by

$$V_m^+ = 2k_n \int_{-T}^{T} I(t') \cos\omega_n t' \, dt' . \quad (28)$$

The retarding potential at the center of such a symmetric bunch is given by

$$V^-(0) = -2k_n \int_{-T}^{0} I(t') \cos\omega_n t' \, dt' = -\frac{1}{2} V_m^+ . \quad (29)$$

If $V^-(0)$ happens also to be the maximum (absolute) value of the retarding potential, then $|V^-(0)| = V_m^-$, and the transformer ratio is $R = V_m^+/V_m^- = 2$. If $V^-(0)$ is *not* at the peak of the retarding potential, then $V_m^- > |V^-(0)|$ and $R < 2$. Thus for symmetric bunches interacting with a single mode, the transformer ratio cannot exceed two. This upper limit is reached only if the maximum retarding potential is reached at the center of symmetry of the distribution. Otherwise, the transformer ratio is less than two. If the bunch is not symmetric, the preceding argument does not apply. The transformer ratio can then in principle be arbitrarily large, as we will see shortly.

Even for symmetric bunches in a physical structure, which has many modes, the limitation $R \leq 2$ tends to apply. For example, Fig. 8 shows potentials for a Gaussian distribution interacting with the SLAC accelerating structure for several values of bunch length. Note that, for a bunch length such that the peak retarding potential is reached near the center of symmetry of the bunch

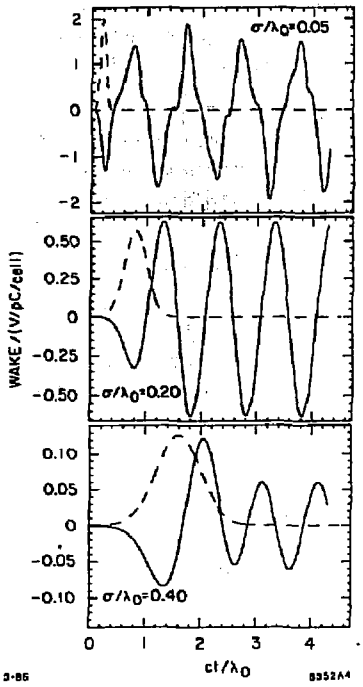

Figure 8. Potential in and behind a gaussian bunch interacting with the longitudinal modes of the SLAC structure. The transformer ratio for $\sigma/\lambda_0 = 0.05$, 0.20 and 0.40 are 1.4, 1.9 and 1.4 respectively.

($\sigma/\lambda_0 = 0.2$), the transformer ratio is approximately equal to two, while for both longer and shorter bunch lengths the transformer ratio is considerably less than two. It can be shown[9] that for a Gaussian bunch interacting with a single mode the loss parameters $k_u \equiv u/q^2$ and $k_a \equiv E_a/2q$ are related to the loss parameter $k_\ell \equiv E_a^2/4u$ by

$$k_u = k_\ell e^{-\omega_n^2\sigma^2/c^2} = k_\ell e^{-4\pi^2\sigma^2/\lambda_n^2} \tag{30a}$$

$$k_a = k_\ell e^{-\omega_n^2\sigma^2/2c^2} = k_\ell e^{-2\pi^2\sigma^2/\lambda_n^2} \tag{30b}$$

for each mode. Thus as the bunch length increases, coupling to higher modes is rapidly suppressed by the exponential factor. For the SLAC structure, $k_\ell p = 0.70$ V/pC/cell for the fundamental mode, where p is the cell length. The amplitude of the accelerating mode voltage per cell excited by a Gaussian bunch with total charge q is therefore

$$\frac{V_1}{q} = 2k_a\, p = 1.40\, e^{-2\pi^2\sigma^2/\lambda_0^2} \qquad \text{V/pC/cell} \quad .$$

For $\sigma/\lambda_0 = 0.05$, 0.20 and 0.40, this gives $V_1/q = 1.33$, 0.64 and 0.08 V/pC/cell. These values agree well with the computer calculation shown in Fig. 8.

The plot for $\sigma/\lambda_0 = 0.4$ in Fig. 8 also illustrates the phenomenon of autoacceleration, in which fields induced by particles at the front of the bunch can accelerate particles at the tail of the same bunch.

It is possible in principle to design a structure in which the accelerating potentials for several modes superimpose maximally at some point behind the bunch to produce $R > 2$. Consider, for example, a two-mode structure with loss factors k_0 and k_1 and frequencies ω_0 and ω_1 related by $\omega_1 = 3\omega_0 + \delta$, where δ/ω_0 is a small quantity (if $\delta = 0$ the maxima of the wakes for the two modes would never superimpose). Assume a rectangular bunch extending from $-T$ to T with constant current $I(t) = I$. From Eq. (22), using also $W_s(t) = 2k_n \cos\omega_n t$, the

retarding potential within the bunch is

$$V^-(t) = -2I\left[\frac{k_0}{\omega_0}\sin\omega_0(t+T) + \frac{k_1}{\omega_1}\sin\omega_1(t+T)\right] \quad . \tag{31a}$$

Behind the bunch ($t > T$),

$$V^+(t) = -4I\left[\frac{k_0}{\omega_0}\cos\omega_0 t\sin\omega_0 T + \frac{k_1}{\omega_1}\cos\omega_1 t\sin\omega_1 T\right] \quad . \tag{31b}$$

If we choose $\omega_0 T = \pi/2$ and $k_1 = k_0$, we find the minimum potential inside the bunch and the maximum potential behind the bunch are

$$V_m^- \approx \frac{8}{3\sqrt{2}}\frac{k_0 I}{\omega_0} \quad \text{and} \quad V_m^+ = \frac{16}{3}\frac{k_0 I}{\omega_0} \quad , \tag{32}$$

and therefore $R \approx 2\sqrt{2}$.

This calculation can be generalized to structures with many modes related by $\omega_n = (2n+1)\omega_0 + \delta_n$. If the loss factors are equal for all of the modes, it is straightforward to show

$$R \approx \left(\frac{8}{\pi}\right)\left(1 + \frac{1}{3} + \frac{1}{5} + \ldots\right) \quad .$$

It can be argued that such a structure is unphysical. On the other hand, there is no reason to believe that the two mode structure described above is not realizable. The $\sqrt{2}$ gain in transformer ratio over the single mode case is, however, quite modest.

Let us now return to the case of an asymmetric driving bunch. Take as an example a triangular current ramp in a single mode cavity. Let $I(t) = I\omega t$ for $0 < t < T$ and $I(t) = 0$ otherwise. For simplicity let the bunch length be

$T = 2\pi N/\omega$, where N is an integer. Then within the bunch

$$V^-(t) = 2kI\omega\int_0^t t'\cos\omega(t-t')\,dt' = -\frac{2kI}{\omega}\,(1-\cos\omega t) \quad , \tag{33a}$$

whereas behind the bunch

$$V^+(t) = 2kI\omega\int_0^T t'\cos\omega(t-t')\,dt' = 2kIT\,\sin\omega t \quad . \tag{33b}$$

Thus $V_m^- = 4kI/\omega$, $V_m^+ = 2kIT = 4\pi kIN/\omega$ and

$$R = \frac{V_m^+}{V_m^-} = \pi N \qquad \left\{\begin{array}{l}\text{current ramp,}\\ \text{single mode}\end{array}\right\} \quad . \tag{34}$$

The wake potentials for a current ramp of length $N = 2$ interacting with a single mode are shown in Fig. 9(a).

In a real structure with many modes, one might expect that the transformer ratio will be less than that given by Eq. (34). The potential excited in the SLAC structure by a current ramp with $N = 2$ is shown in Fig. 10. Within the bunch the retarding potential has a behavior close to the single mode calculation, $V^-(t) \sim 1 - \cos\omega t$. However, some energy goes into higher modes, as is evident by ripples on the cosine wave behind the bunch. This causes a degradation of the transformer ratio from the single mode prediction $R = 2\pi$ to $R = 4.86$. The degradation worsens as the bunch gets longer, as can be seen in Fig. 11.

The efficiency for energy extraction from a driving bunch extending from $t = 0$ to $t = T$ in which all of the electrons have the same energy $eV_0 = eV_m^-$ is

$$\eta = -\frac{1}{qV_m^-}\int_0^T I(t)\,V^-(t)\,dt \quad . \tag{35}$$

For a linear current ramp interacting with a single mode, substitution of Eq. (33a) together with appropriate expressions for $I(t)$, V_m^- and q into Eq. (35) gives an

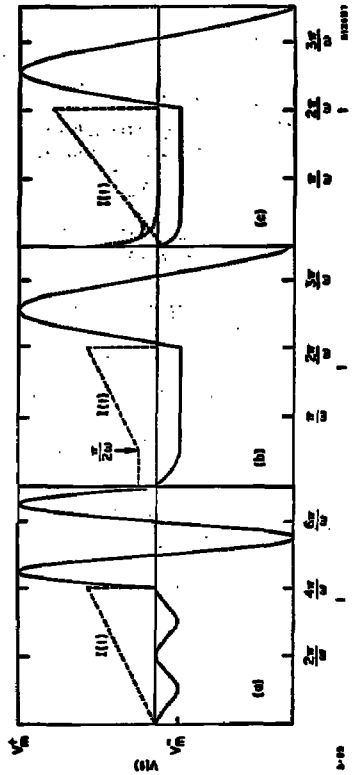

Figure 9. The voltage induced by three different asymmetric current distributions interacting with a single mode.

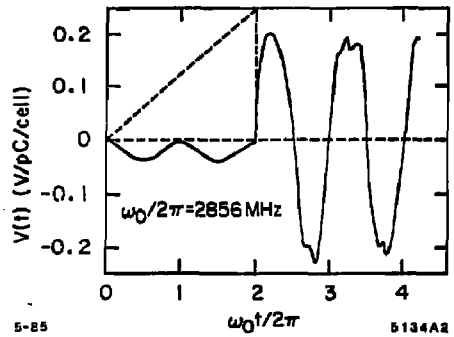

Figure 10. The potential induced by a linear current ramp interacting with the modes in the SLAC structure.

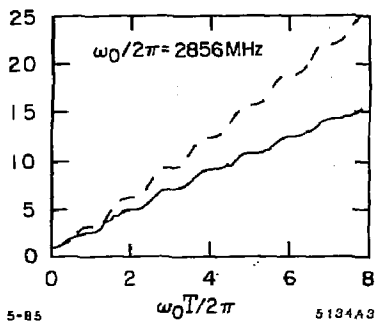

Figure 11. The transformer ratio for a linear current ramp in the SLAC structure as a function of bunch length. The dashed line gives single mode results.

efficiency of 0.5 if $\omega T = 2\pi N$. A higher efficiency and a higher transformer ratio could be obtained if the retarding potential could be made as flat as possible across the current distribution. In the limit $V^-(t) = V_m^- = \text{constant}$, Eq. (35) gives an efficiency of 100%. In Ref. 12 it is proven that the potential can be exactly flat only for a current distribution which consists of a delta function followed by a linear current ramp, where the proper relation exists between the value of the delta function and the slope of the current ramp. In this limit the transformer ratio is given by[12]

$$R = \left[1 + (2\pi N)^2\right]^{1/2} \qquad \left\{ \begin{array}{c} \text{Delta function plus} \\ \text{current ramp,} \\ \text{single mode} \end{array} \right\} . \tag{36}$$

Here $N = \omega T/2\pi = cT/\lambda$, and N can now take non-integer values. For large N the transformer ratio approaches $R \approx 2\pi N$ and the efficiency approaches 100%. The transformer ratio for the delta function alone ($N \to 0$) is $R = 1$, as we know is the case for all short bunches, and the efficiency is 0.5. An approximation to this distribution, in which the wake potential is driven negative by an exponentially decaying spike and then held constant by a rising current ramp, is illustrated in Fig. 9(c).

A third distribution of interest is a linear current ramp preceded by a quarter wavelength rectangular pulse. The response to this distribution is shown in Fig. 9(b). The transformer ratio in the case of this "doorstep" distribution is[12]

$$R = \left[1 + \left(1 - \frac{\pi}{2} + 2\pi N\right)^2\right]^{1/2} \qquad \left\{ \begin{array}{c} \text{Doorstep plus} \\ \text{current ramp,} \\ \text{single mode} \end{array} \right\} . \tag{37}$$

In the limit of large N the transformer ratio again approaches $R \approx 2\pi N$. For long bunches the transformer ratio and the efficiency are again approximately twice that for the linear current ramp alone. Except for particles in the first quarter wavelength of the bunch, all particles experience the same retarding potential. At the end of the doorstep ($N = 1/4$), $R = \sqrt{2}$ and $\eta = 2/\pi$.

As a numerical example, consider an accelerator operating at $\lambda = 1$ cm with a desired gradient of 200 mV/m. A SLAC-type structure at this wavlength would have a loss parameter on the order 2×10^{15} V/C-m. With a transformer ratio of 20, driving bunches with an energy of 100 MeV would need to be injected every ten meters. The charge per bunch as given by Eq. (4) is

$$q = \frac{E_a R}{4k\eta} \approx 0.5\ \mu C \quad ,$$

assuming that most of the energy goes into a single mode and that the efficiency is close to 100%. The bunch length is approximately $R\lambda/2\pi = 3.2$ cm or 100 ps, and the peak current at the end of the bunch is 10 kA. Many practical questions must be addressed, such as the feasibility of creating properly shaped bunches with very high peak currents. The deflecting fields induced if the driving bunch wanders off the axis of the structure are also a serious problem.

5. Ring Beams in Cylindrically Symmetric Structures

In this section we consider cylindrically symmetric structures excited by a beam in the form of a ring, or hollow cylinder with thin "walls". A simple case for which the beam-structure interaction can be computed analytically is the pillbox cavity having a thin azimuthal slot at radius r_0, as shown in Fig. 12. If the slot is located near the outer perimeter of the cavity, we might expect a large transformer ratio. In qualitative terms, a driving bunch entering the cavity generates a wave packet which travels toward the axis. The volumn of the wave packet decrease roughly as r^{-1}, and the electric and magnetic field strengths must therefore increase approximately as $r^{-1/2}$. A second bunch can then be accelerated along the axis of the cavity. In a practical structure, the effect of the axial beam tube and the azimuthal slot on the wake potentials must be taken into account.

The advantage of a ring beam over a line beam at the same radius is that higher order azimuthal modes ($m > 0$) are not excited. Since a ring beam

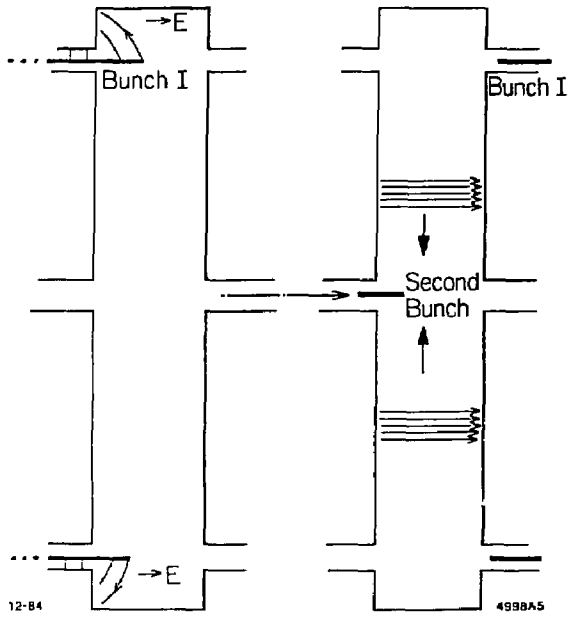

Figure 12. Qualitative picture of the field induced by a ring bunch passing through a pillbox cavity.

is a superposition of an infinite number of line beams at the same radius, the transformer ratio for a ring beam with radius r_0 and a line beam at radius r_0 with the same axial charge distribution would be the same if azimuthally varying modes are ignored. Inclusion of these modes would degrade the transformer ratio, and in addition a deflecting wake would be generated on the axis of the pillbox.

If only the lowest frequency TM_{010} mode in a pillbox cavity is excited by the ring driving bunch, the transformer ratio for a ring bunch with axial extent $\Delta z = 0$ can be obtained from Eq. (20a) as

$$R = 2\left[\frac{k(0)}{k(r_0)}\right]^{1/2} = \frac{2}{J_0(p_{01}r_0/b)} \tag{38}$$

where b is the outer radius of the cavity and $p_{01} = 2.405$ is the first root of J_0. In practice, a long bunch excites predominately the lowest frequency mode. For a flat current distribution (rectangular bunch) of length Δz, Eqs. (31a) and (31b) can be used to show that the above transformer ratio must be multiplied by a bunch form factor

$$F = \frac{\sin(\pi\,\Delta z/\lambda_0)}{\sin(2\pi\,\Delta z/\lambda_0)}\,, \qquad \frac{\Delta z}{\lambda_0} < \frac{1}{4}$$
$$F = \sin(\pi\,\Delta z/\lambda_0)\,, \qquad \frac{\Delta z}{\lambda_0} > \frac{1}{4} \tag{39}$$

where λ_0 is the wavelength of the fundamental mode. Mitrovich *et al.*[13] have computed the energy going into higher modes for a pillbox cavity with $g/\lambda_0 = 0.1$ and $\Delta z/\lambda_0 = 0.425$ as a function of the beam radius r_0. For this driving bunch length, more than 90% of total energy deposited in all modes goes into the fundamental mode for $0.15 < r_0/b < 0.72$. At the upper end of this range, the transformer ratio is 5.1. Higher transformer ratios could of course be reached by making r_0/b closer to one. However, more energy then goes into higher modes. In addition, the driving bunch distribution could be shaped, as discussed in the previous section.

A wake field "transformer," which consists essentially of a series of pillbox cavities with a ring gap near the outer radius and a hole on the axis for the accelerated beam, has been proposed by Voss and Weiland.[14,15] An experiment[16,17] is in progress at DESY to test the concept by injecting an 8 MeV, 1 μC beam into the structure shown schematically in Fig. 13. Also shown are the wake fields calculated at eight time steps by T. Weiland using his code TBCI.[18] Note that the outer boundary of the structure has been shaped to enhance the transfer of energy into the radially propagating wake fields. After the wave reaches the axis it is reflected and travels back to the outer boundary. There it is reflected once again, travels back to the axis, and produces a second high field pulse. This second pulse has the inverse sign and can be used to accelerate positrons.

Figure 14 shows the longitudinal potential due to these fields for the driving beam and for an accelerated beam on the axis. The maximum decelerating wake potential seen by the particles in the driving beam is computed to be 17 mV/m, but on the axis a gradient of 170 mV/m is produced. Thus the transformer ratio for this particular structure is 10.

Some important observations can be made concerning the deflecting wake fields in the driving beam. For the usual cavity with no metal between the beam and the axis, recall that the dipole wake potential can be written as

$$c\int \mathbf{F}\,dt = \hat{\mathbf{r}}\,W_r(s)\,\cos\phi + \hat{\boldsymbol{\phi}}\,W_\phi(s)\,\sin\phi = W_\perp(s)\left(\hat{\mathbf{r}}\,\cos\phi - \hat{\boldsymbol{\phi}}\,\sin\phi\right)\,,$$

where $W_r(s) = -W_\phi(s)$. We now find, when there is metal between a hollow beam and the axis, that the deflecting forces cannot be described by a single transverse wake function.[18] Two functions are now required at a given fixed radius for the ring beam (and four if the position of the ring beam is allowed to vary):

$$c\int \mathbf{F}_\perp(r,\phi)\,dt = \hat{\mathbf{r}}\,W_r(s)\,\cos\phi + \hat{\boldsymbol{\phi}}\,W_\phi(s)\,\sin\phi\,,$$

where $W_r(s) \neq -W_\phi(s)$. As an example, Fig. 15 shows the dipole wake potentials for the inner bunch ($W_r = W_\phi$) and the outer bunch ($W_r \neq -W_\phi$) for the

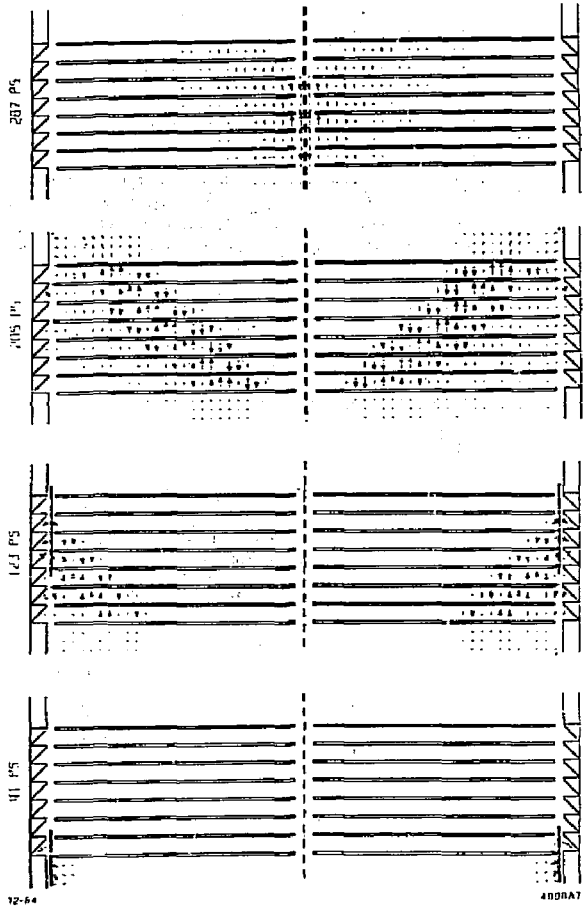

Figure 13. Electric field at eight time steps generated by a hollow driving beam in a seven-cell pillbox transformer.

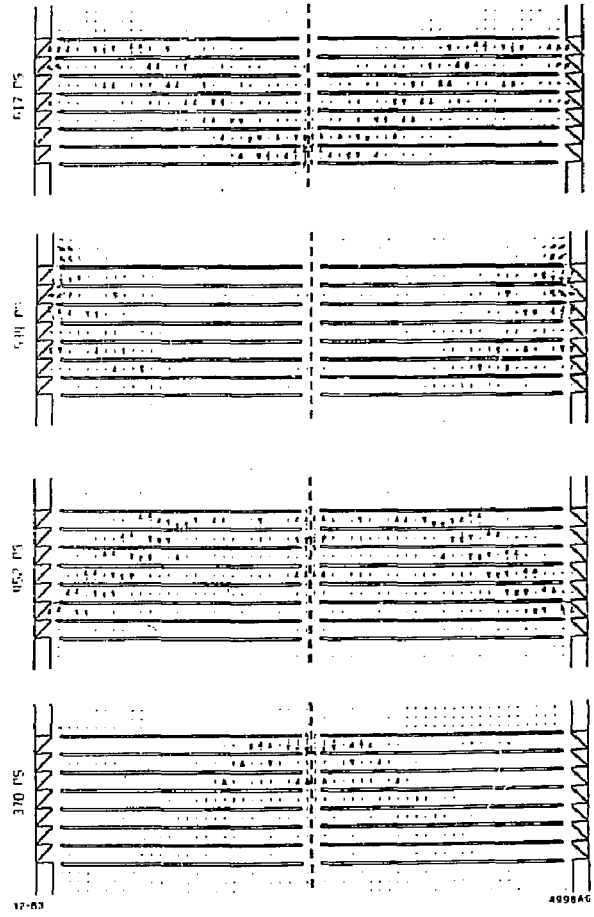

Figure 13 (Continued)

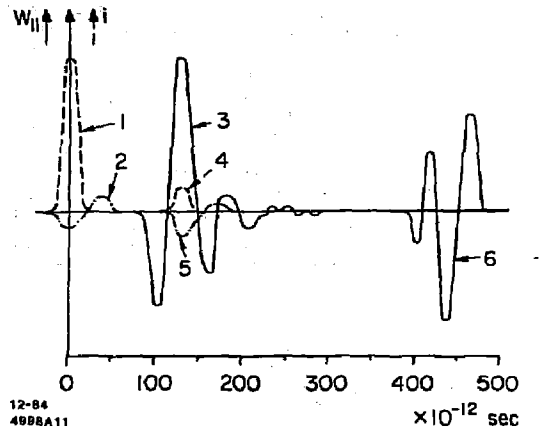

Figure 14. Longitudinal potential for the wake field transformer shown in Fig. 13. (1) Driving beam density; (2) decelerating potential inside driving beam; (3) accelerating potential on axis; (4) density of the accelerated beam; (5) self potential of the accelerated beam; (6) accelerating potential after reflection from outer wall.

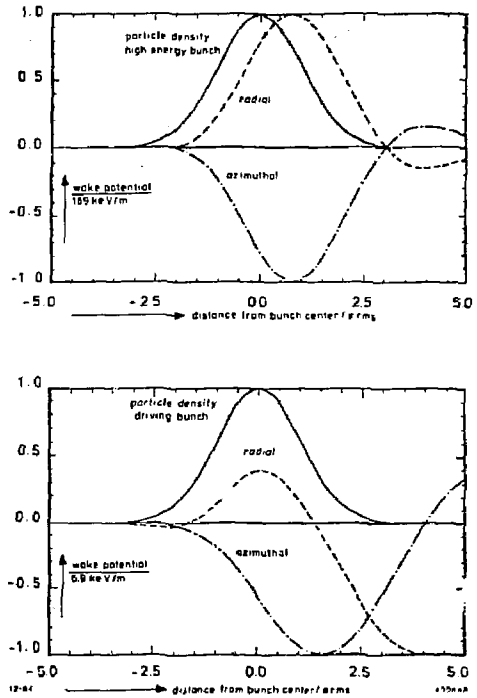

Figure 15. Transverse wake potential on the axis (top) and at the outer driving ring beam (bottom) generated by a 0.1 mm offset of the driving beam in the structure shown in Fig. 13. The parameters of the driving beam are $\sigma_z = 2$ mm, $Q = 1\ \mu C$ and $r_0 = 5$ cm.

structure in Fig. 13. This behavior of the wake potentials makes the study of beam dynamics in the driving bunch much more complicated. A related result is also of importance for such structures: cylindrically symmetric fields ($m = 0$ modes) can deflect. This is not the case for the more usual single-region cavities.

Other structures have been proposed[14,15] which do not need a hollow driving beam, for example the elliptical structure shown in Fig. 16 and the multi-beam star-transformer shown in Fig. 17. In the elliptical geometry one makes use of the property that the peak wake potential depends on the size of the beam hole. In the star transformer wake fields from the driving beams propagate toward the axis and combine in a straightforward manner. A transformer ratio on the order of $2N$, where N is the number of driving beams, might be expected.

An experiment at Osaka University[19] using the elliptical wake field transformer has already been performed. The computed transformer ratio in this experiment is 1.3. The deflecting wake fields for this structure have also been computed,[20] and were found to be very high ($\sim 1/3$ of the accelerating field).

ACKNOWLEDGEMENTS

In writing these lecture notes, liberal use has been made of material in Refs. 6 and 12. I am indebted to coauthors K. Bane, P. Chen and T. Weiland for relying heavily on work to which they have contributed so substantially. In particular, Sec. 3 on wake potentials in closed cavities is based largely on K. Bane's analysis which was first reported in Ref. 7. I would also like to thank K. Bane for computing the curves shown in Fig. 8.

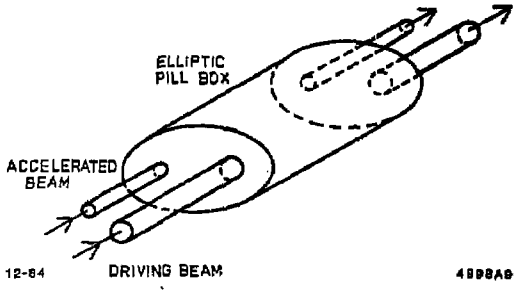

Figure 16. Two-beam elliptical pillbox acting as a wake field transformer.

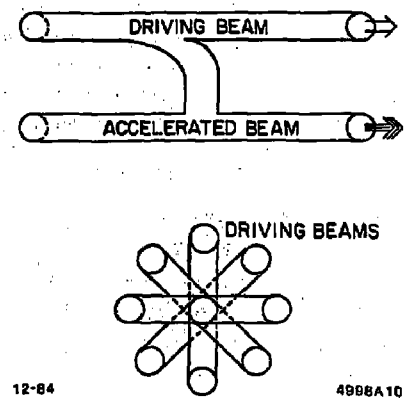

Figure 17. A multiple-beam star transformer.

REFERENCES

1. R.D. Ruth and Pisin Chen, *Plasma Aeeelerators*, these Proceedings. Also SLAC-PUB-3906, March 1986.
2. K. Satoh, private communication.
3. A.W. Chao, PEP-Note-332, SLAC, June 1980.
4. A.W. Chao and P.L. Morton, *PEP-Note-105*, SLAC, 1975.
5. K. Bane, private communication. See also T. Weiland and B. Zotter, Part. Accel. 11, 143 (1981).
6. K.L.F. Bane, P.B. Wilson and T. Weiland in *Physics of High Energy Particle Accelerators*, BNL/SUNY Summer School, 1983, M. Month, P. Dahl and M. Dienes, eds., AIP Conference Proceedings No. 127 (American Institute of Physics, New York, 1985), pp. 875-928. Also SLAC-PUB-3528, December 1984.
7. K. Bane, CERN/ISR-TH/8-47, 1980.
8. W.K.H. Panofsky and W.A. Wenzel, Rev. Sci. Instrum. 27, 967 (1956).
9. P.B. Wilson in *Physics of High Energy Particle Accelerators*, Fermilab Summer School, 1981, R.A. Carrigan, F.R. Huson, M. Month, eds., AIP Conference Proceedings No. 87 (American Institute of Physics, New York, 1982), Sec. 6.1. Also SLAC-PUB-2884, February 1982.
10. See for example R.E. Collin, *Foundations for Microwave Engineering* (McGraw-Hill, New York, 1966), Sec. 2.12.
11. K. Bane and P.B. Wilson, *Proceedings of the 11th International Conference on High-Energy Accelerators*, CERN, July 1980 (Birkhäuser Verlag, Basel, 1980), p. 592.
12. K.L.F. Bane, Pisin Chen and P.B. Wilson, IEEE Trans. Nucl. Sci. NS-32, No. 5, 3524 (1985). Also SLAC-PUB-3662.

13. D. Mitrovich *et al.*, IEEE Trans. Nucl. Sci. NS-30, No. 4, 3518 (1983).

14. G.A. Voss and T. Weiland, DESY M-82-10, April 1982.

15. G.A. Voss and T. Weiland, DESY 82-074, November 1982.

16. The Wake Field Accelerator Study Group, DESY M-83-27, 1983; and *Proceedings of the 12th International Conference on High Energy Accelerators*, Fermilab, 1983, p. 454.

17. T. Weiland, IEEE Trans. Nucl. Sci. NS-32, No. 5, 3471 (1985).

18. T. Weiland, DESY 82-015, 1982; and Nucl. Instrum. Methods 212, 131 (1983).

19. S. Takeda, Osaka University, private communication.

20. Y. Chin, KEK 83-19, 1983.